International Journal of Technology 11(4) 842-851 (2020)
Received June 2020 / Revised July 2020 / Accepted August 2020

International Journal of Technology

http://ijtech.eng.ui.ac.id

Utilization of Dammar-Gum as a Soft Template in Titania Synthesis for Photocatalyst

Salprima Yudha S[1]*, Aswin Falahudin[1], Asdim[1], Jeong In Han[2]

[1]*Department of Chemistry, Faculty of Mathematics and Natural Sciences, Universitas Bengkulu, Jalan W.R. Supratman, Kandang Limun, Bengkulu 38371, Indonesia*
[2]*Department of Chemical and Biochemical Engineering, Dongguk University-Seoul 30, Pildong-ro 1 gil, Jung-gu, Seoul 04620, Republic of Korea*

Abstract. A new synthetic method for the preparation of titania (TiO_2) was developed. The synthesis involved utilizing dammar gum as the natural soft template, chloroform ($CHCl_3$) as the reaction solvent, and titanium tetraisopropoxide (TTIP) as the main precursor. The results show that the methodology described herein is an efficient alternative for the preparation of titania with larger surface areas up to 58.1 $m^2\ g^{-1}$ for TiO_2 from the TTIP-dammar gum/$CHCl_3$/H_2O reaction system, and 56.2 $m^2\ g^{-1}$ for TiO_2 from the TTIP-dammar gum/$CHCl_3$ reaction system. Both surface areas are larger than that of the pure TTIP/$CHCl_3$/H_2O product (5.56 $m^2\ g^{-1}$). In addition, the as-prepared TiO_2, which uses dammar gum as a soft template, exhibited higher photocatalytic activity toward rhodamine B degradation compared to the as-prepared TiO_2 in the absence of dammar gum.

Keywords: Dammar-gum; Photocatalyst; Soft template; Titania

1. Introduction

Owing to its remarkable physical and chemical properties, titanium dioxide (TiO_2) or titania, is well known as one of the most desired semiconductor materials. It is known that all phase types of titania (anatase, rutile, and brookite) are effective as photocatalysts under ultra-violet (UV) light irradiation (Jing et al., 2011). A number of synthetic approaches for TiO_2 have been reported widely (Slamet et al., 2017; Kusrini et al., 2019). A popular and efficient strategy includes development of this material on various templates (Xie et al., 2016; Niu et al., 2018). For instance, application of resorcinol-formaldehyde resin as a template for the preparation of a TiO_2 hollow nanostructure has recently been described. It has been shown that hollow titania has good activity as a photocatalyst for the degradation of rhodamine B under UV radiation. This result indicates that the hollow titania structure is important for its catalytic activity (Tang et al., 2013). Alginate has also been claimed as a good sacrificial soft template for the synthesis of specific pores and nanoparticles. In particular, the role of alginate as a template for nucleation and the formation of porous TiO_2 has been described (Yu et al., 2016).

---

*Corresponding author's email: salprima@unib.ac.id or sp.yudha.s@gmail.com, Tel.: +62-736-20919
doi: 10.14716/ijtech.v11i4.4162

Other methods of obtaining mesoporous TiO_2 include reacting titanium isopropoxide in the presence of a semi-rigid template, such as a rod-shaped virus bacteriophage, M13. TiO_2 was obtained using this methodology and was shown to exhibit good stability, particularly in the anatase phase when the calcination temperature elevated to 800°C (Hernández-Gordillo et al., 2018). Furthermore, the poly(butyl methacrylate) (PBMA) colloidal crystal template has also been developed to synthesize titania using a sol-dipping template method. The TiO_2 that was obtained using this procedure was shown to have a meso-scale pore structure, which was indicated by the many holes that were formed following the calcination procedure used to remove the template (Zhang et al., 2012).

Other research shows that utilizing different bio templates results in the formation of different crystal phases of TiO_2, even at calcination temperatures of up to 750°C. TiO_2 was obtained in the anatase phase when albumen and yeast were used as templates. In contrast, when dandelion pollen was utilized, only the rutile phase was isolated (Bao et al., 2012). A variety of concentrations of rice straw (lignocellulosic waste material) were investigated as soft templates when using the sol-gel methodology. A synthetic modification procedure was carried out to alter the pore volume and size of the TiO_2 (Ramimoghadam et al., 2014).

However, the use of natural templates is not only restricted to soft templates. For instance, mesoporous crystalline TiO_2 was synthesized using silica KIT-6. The synthetic procedure involved the addition of NaOH to remove the silica template from the desired material (Zhang et al., 2010). Furthermore, a different strategy used pluronic polymeras as the template. A further advantage of using this material was its photocatalytic activity in photo-degradation of orange II under UV irradiation and inert conditions (Xiong et al., 2010). More recently, the synthesis of TiO_2 from tetrabutyl titanate was carried out using cotton as a hard template. The annealing temperature was 600°C (2 hours), which afforded the anatase phase of TiO_2 (Wang et al., 2015). Other research has shown that TiO_2 nanoparticles can be synthesized using polyamidoamine (PAMAM) dendrimer molecules as a template (Peng et al., 2016).

Moreover, it has been demonstrated that combining two or more templates can increase the activity of the obtained titania. The synthesis of a grain size of TiO_2 nanotubes, using anodic aluminum oxide membrane as a hard template and a complex of polystyrene-block-polyethylene oxide with titanium isopropoxide, has recently been reported. It was demonstrated that the field emission performance was dependent on the grain size of the TiO_2 (Yang et al., 2017). A sol-gel agent made from acrylic acid and N,N'-methylenebis(acrylamide) was also used to synthesize titania, which resulted in the formation of anatase and rutile phases in various ratios. The obtained products were tested as cathode materials for use in a rechargeable aqueous aluminum-ion battery (Ojeda et al., 2017). Furthermore, the common surfactant, cetyltrimethylammonium bromide, was combined with the P123 polymer as a medium to synthesize of TiO_2. The synthetic procedure involved using titanium tetrachloride as the precursor and heating the reaction mixture to 550°C for 3 h. The method resulted in the formation of a crystalline rutile phase (Liu et al., 2018).

Biotemplates have not only been used to prepare metal oxides but have also been used as composite precursors. An example of this is the synthesis of porous hierarchal spirulina/TiO_2 composite, which resulted in the enhancement of their photocatalytic activity (Tu et al., 2012). Other results show that nanofibril-interconnected cellulose aerogel could be used as a biotemplate for the synthesis of hierarchical porous TiO_2 with a highly specific surface area (Zhang et al., 2017). In addition, the use of kenaf fiber as a sacrificial template produced nanostructured tubular TiO_2 (Osman et al., 2018).

Currents research shows that dammar gum can be used as a micro-encapsulating material for drugs, such as diltiazem hydrochloride and ibuprofen, using the oil-in-oil emulsion solvent evaporation technique. It was demonstrated that encapsulation efficiency increased as the dammar gum content increased. Unfortunately, the release rates of the drugs was reduced (Morkhade and Joshi, 2007). It is known that the materials desired for photocatalysis and photoelectrode purposes possess two common characteristics: crystallinity and large surface areas (Zhang et al., 2010; Nursama and Muliani, 2012). In this study, a green, two-step approach for the fabrication of titania was developed using natural dammar gum as a bio-template, without the addition of bases, such as NaOH, NH_4OH, KOH, or others. Our simple methodology could be used as an alternative to synthesize TiO_2. The dammar gum was used as a new bio-template for the complexation of the titanium (IV) isopropoxide (TTIP) precursor, in order to synthesize TiO_2. Furthermore, the synthesized TiO_2 that used dammar gum as the soft template had high photocatalytic activity for rhodamine B degradation.

2. Methods

2.1. Materials

Chloroform was purchased from Merck (Germany) and titanium-tetraisopropoxide was obtained from Sigma-Aldrich (Germany). All of the reagents were used without further purification. Demineralized water was used in all of the reported experiments. Finally, dammar gum was obtained from a local traditional market in Bengkulu.

2.2. Experimental Procedure and Product Characterization

Three types of reaction systems were developed: (1) TTIP/$CHCl_3$/dammar gum/H_2O; (2) TTIP/$CHCl_3$/dammar gum; and (3) TTIP/$CHCl_3$/H_2O. The TTIP/$CHCl_3$/dammar gum/H_2O reaction was developed as follows: A solution of dammar gum was prepared by adding dammar gum powder (5 g) to $CHCl_3$ (50 mL). The solution was then stirred using a magnetic stirrer for 30 minutes before adding titanium isopropoxide (5 gram). The reaction mixture was stirred again for 1 hour at room temperature under aerobic conditions. Demineralized water (100 mL) was added under vigorous stirring at room temperature over 30 minutes. The mixture was then allowed to react at room temperature for 4 days, after which a gel formed during the organic phase. The gel was separated, dried at 120°C for 2 hours and calcinated at 500°C for 4 hours. The TTIP/$CHCl_3$/dammar gum reaction was developed using the same procedure without adding H_2O. Finally, the control sample (TTIP/$CHCl_3$/H_2O) was synthesized using the same procedure without the addition of dammar gum powder, and chloroform (5 g) was used as a dammar gum substitute.

The crystalline phases of TiO_2 were characterized by X-ray Diffraction (XRD) using X'PERT Powder-PANalytical PW 30/60. The acquisition parameters were scan axis: gonio; scan type: continuous; PSD mode: scanning; divergence slit type: fixed; divergence slit size (°): 0.8709; specimen length (mm): 10.00; measurement temperature (°C): 25.00; anode material: Cu; K-alpha1 (A°): 1.54060; K-alpha2 (A°): 1.54443; K-beta (A°): 1.39225; K-A2/K-A1 ratio: 0.50000; generator settings: 30 mA, 40 kV.

The morphology of the obtained TiO_2 was investigated by Scanning Electron Microscopy (SEM) and the chemical composition of the TiO_2 powder was determined by Energy Dispersive X-ray (EDX) analysis using JEOL JSM 6510 LA. The acquisition parameters were Acc. voltage: 20.0 kV; energy range: 0–20 keV; real time: 51.41–51.49 sec; live time: 50.00 sec; dead time: 2%; counting rate: 2910–3205 cps.

The surface areas and pore sizes of the synthesized TiO_2 samples were determined using Brunauer-Emmett-Teller (BET) and Barret-Joyner-Halender (BJH) analyses, which were based on the N_2 adsorption and desorption isotherms using a Quantachrome® ASiQwin™ analyzer. The acquisition parameters were as follows: analysis mode: standard; analysis gas: nitrogen; voldvol: He measure; outgas temperature: 300°C; batch temperature: 77.35°C; cell type: 9 mm w/o rod.

The photocatalytic degradation of rhodamine B (RhB) was investigated in a 10 ml sample bottle containing RhB solution (5 ppm, 5 mL) and a TiO_2 sample (25 mg; 0.312 mmol). The suspension was kept in the dark for 30 minutes to achieve the adsorption-desorption equilibrium of the dye before illumination. After irradiation with sunlight for 3 hours (12:00 a.m. – 3:00 p.m.), an aliquot was taken for further analysis. The RhB concentration of the solution was analyzed using optical absorption (Agilent 60 spectrophotometer) at 554 nm.

3. Results and Discussion

Titanium dioxide (TiO_2) particles were fabricated using dammar gum as a soft template in $CHCl_3$. Our methodology used three reaction conditions. First, the control conditions were developed by adding titanium tetraisopropoxide (TTIP) solution without the presence of dammar gum (TTIP/$CHCl_3$/H_2O). Second, the main reaction conditions were investigated in the presence of dammar gum followed by the addition of water (TTIP-dammar gum/$CHCl_3$/H_2O). Third, the other reaction conditions were investigated in the presence of dammar gum without the addition of water (TTIP-dammar gum/$CHCl_3$). Figure 1 presents images of all three reaction flows.

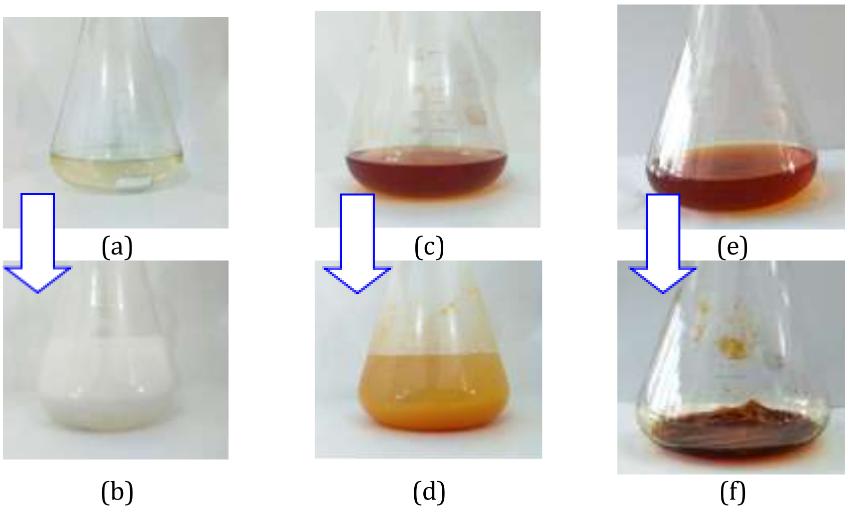

Figure 1 Chart flow of the TiO_2 synthesis: (a) reaction of TTIP in $CHCl_3$; (b) reaction of TTIP in $CHCl_3$ after the addition of an excess of demineralized water; (c) reaction of TTIP and dammar gum in $CHCl_3$; (d) reaction of TTIP and dammar gum in $CHCl_3$ after the addition of demineralized water; (e) reaction of TTIP and dammar gum in $CHCl_3$ without the addition of water; (f) reaction system after the $CHCl_3$ solvent evaporated.

When the control conditions (TTIP/$CHCl_3$/H_2O) were used, the TTIP dissolved homogenously to form a transparent solution (Figure 1a). However, following the addition of demineralized water in excess, a white gel formed in the aqueous layer (Figure 1b). In contrast, the reaction for TTIP-dammar gum/$CHCl_3$/H_2O was performed under the same temperature but in the presence of dammar gum, which resulted in the formation of a homogenous brown solution (Figure 1c). Furthermore, a deep yellow gel was formed following the addition of demineralized water (Figure 1d). Interestingly, the gel was observed in the organic, rather than in the aqueous, phase. These results indicated that the presence of dammar gum altered the solubility of the corresponding intermediate due to the formation of the Ti-dammar gum complex compound. The gel materials were then heated at 120°C for 2 hours, followed by heating at 500°C for 4 hours using a furnace in order to remove the organic materials and obtain the desired TiO_2 product. The other experiment followed the same procedure for the TTIP-dammar gum/$CHCl_3$ (Figure 1e) without the addition of water, followed by direct evaporation of the $CHCl_3$ solvent to form a deep brown gel (Figure 1f) followed by calcination at the same temperature. The phase compositions, as well as the crystal size of all the as-prepared TiO_2 samples were studied through XRD analysis. Figure 2 presents the results of the analyses.

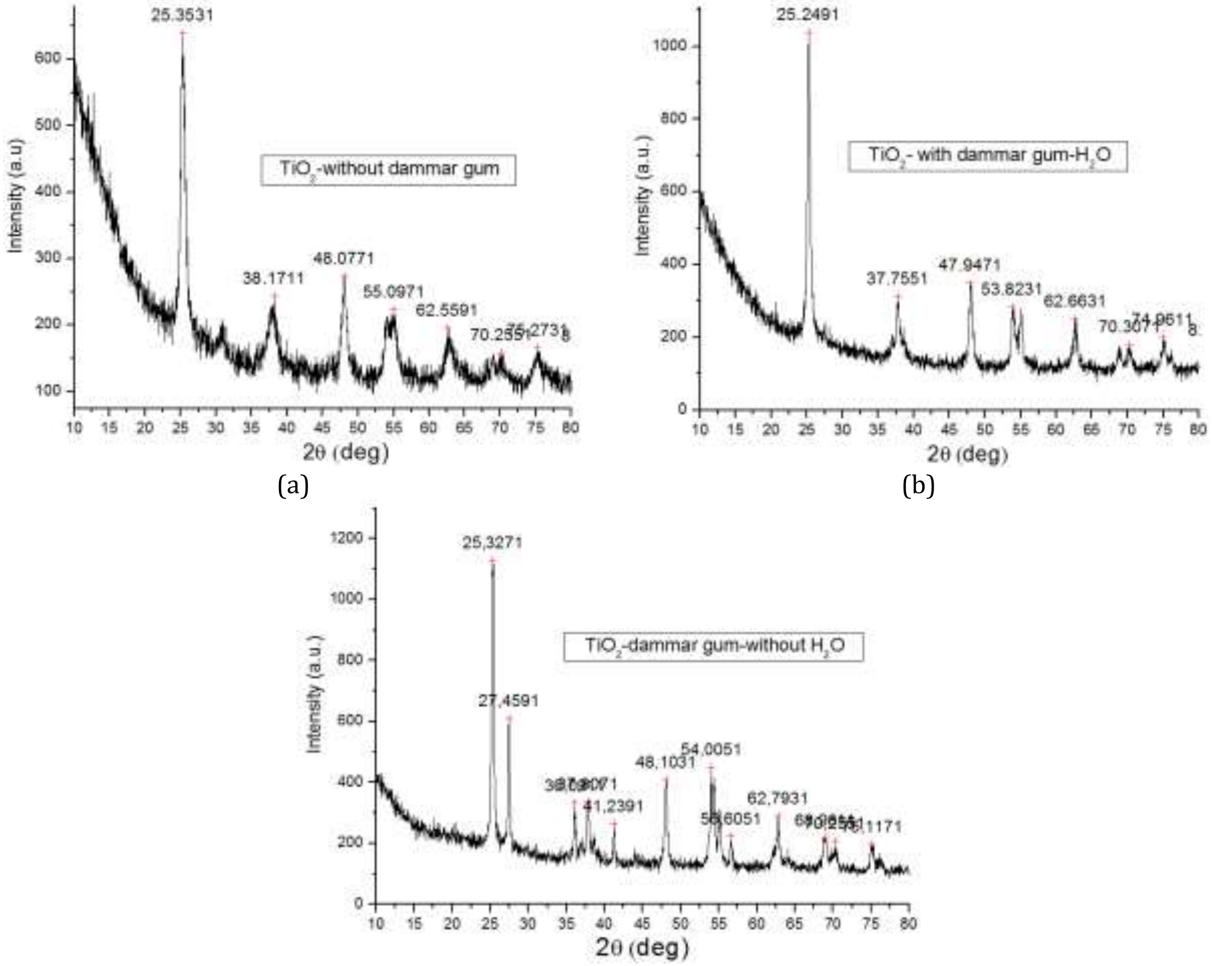

(a) (b)

(c)

Figure 2 XRD pattern of TiO_2: (a) product obtained from the (TTIP/$CHCl_3$/H_2O) reaction system after calcination; (b) product obtained from the TTIP-dammar gum/$CHCl_3$/H_2O reaction system with the addition of water and after calcination; (c) product obtained from the TTIP-dammar gum/$CHCl_3$ reaction system without the addition of water and after calcination

Figure 2a shows the XRD profiles of the gel sample that was obtained from the TTIP/$CHCl_3$/H_2O system after heating at 120°C for 2 hours and calcination at 500°C for 4 hours. The appearance of some broad diffraction peaks located at 25.3°, 38.2°, 48.1°, and 55.1° indicate the presence of TiO_2 (anatase phase), as well as some amorphous materials in the mixture. In contrast, the formation of more crystalline TiO_2 was observed in the second reaction condition (TTIP-dammar gum/$CHCl_3$/H_2O), which was demonstrated by the appearance of sharp peaks at 25.3°, 37.8°, 47.9°, and 53.8° (Figure 2b). In general, diffractional peaks were observed for all of the final samples are in good agreement with standard JCPDS: 21-1272 (Scarpelli et al., 2018). On the other hand, when the reaction of TTIP-dammar gum/$CHCl_3$ was conducted with calcinations in the same condition and without the addition of water, the XRD diffractogram showed new peaks of 27.5°, 36.1°, 41.2°, and 56.6°, which corresponds to the rutile structure along with the anatase TiO_2 peaks (Figure 2c). The obtained anatase/rutile composite in the current condition revealed that the anatase-to-rutile phase transformation could occur at 500°C. The current result indicated that adding dammar gum in the absence of water provoked the phase transformation from anatase to rutile through the exothermic decomposition of the titanium-dammar gum complex, which created high temperatures during the calcination process. Previous research showed that the phase transition of TiO_2 from anatase to rutile initially occurred at 600°C (Ibrahim et al., 2017). The mean crystal sizes of Figures 2a, 2b, and 2c were calculated from the full width at half maximum (FWHM) using the Debye-Scherrer formula (Yang et al., 2017). The results showed that titania samples from the reaction system of all conditions have similar mean crystal sizes of approximately 1.5–3.0 A°.

Figures 3a, 3b, and 3c present the morphologies of the titania produced from reactions in the absence and in the presence of the soft template in $CHCl_3$, respectively. There was significant differences in the morphologies of the TiO_2 obtained from the TTIP-dammar gum/$CHCl_3$/H_2O (Figure 3b) and the TTIP-dammar gum/$CHCl_3$ reactions (Figure 3c) compared to the titania produced in the TTIP/$CHCl_3$/H_2O reaction (Figure 3a). However, the incorporation of dammar gum into the intermediate compound before calcination resulted in a TiO_2 product with a coarse surface.

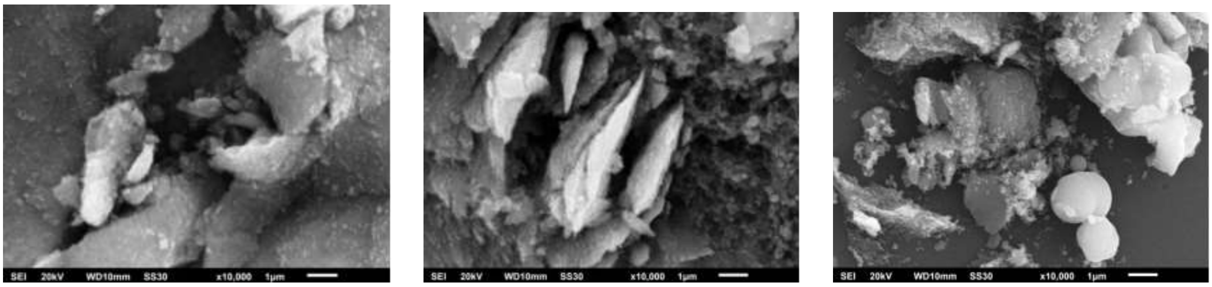

(a) (b) (c)

Figure 3 SEM pattern of calcined TiO_2 product obtained from: (a) the TTIP/$CHCl_3$/H_2O reaction system; (b) the TTIP-dammar gum/$CHCl_3$/H_2O reaction system; and (c) the TTIP-dammar gum/$CHCl_3$ reaction system

The EDX analysis was carried out on samples from the three reactions described above (Table 1) in order to further confirm the formation of TiO_2. The EDX results indicate the presence of oxygen and titanium as major elements. The first two elements predominate the sample, as shown by the mass percentage and a simple stoichiometry calculation. The molecular ratio of the Ti:O in all of the reaction systems approached 1:2 and provided more evidence that the current reaction systems produced the desired titania (TiO_2) in high purity.

Table 1 EDX data of calcined TiO_2 product obtained from three reaction systems

Reaction System	Mass%					Mole	
	Ti	O	C	Si	Zr	Ti	O
$TTIP/CHCl_3/H_2O$	55.32	37.26	6.61	-	0.81	1.156	2.329
$TTIP/CHCl_3$/dammar gum/H_2O	56.59	38.50	4.32	0.59	-	1.182	2.406
$TTIP/CHCl_3$/dammar gum	59.93	40.07	-	-	-	1.252	2.505

These results are in line with the reported EDX data (Ba-Abbad et al., 2012), although some minor impurities (silicon, zirconium and carbon) were detected during our analysis.

The Brunauer-Emmett-Teller (BET) surface area of the products of the TTIP-dammar gum/$CHCl_3/H_2O$ reaction system was 58.1 m^2 g^{-1}, and 56.2 m^2 g^{-1} for the productions of the TTIP-dammar gum/$CHCl_3$ reaction system. Both surface areas were larger than that of the pure $TTIP/CHCl_3/H_2O$ product (only 5.56 m^2 g^{-1}). These results show that the surface area of the TiO_2 was affected by the incorporation of the dammar gum to the titanium oxide precursor, either as a matrix or a complexation agent. The surface area of the TiO_2 obtained from the reaction systems in the presence of the dammar gum was similar to that of the TiO_2 reported by other researchers (Zulmajdi et al., 2020). On the other hand, the Barret-Joyner-Halender (BJH) pore size distribution analysis show that the average pore size was not much different in products from reaction systems that used dammar gum compared to those without dammar gum. The pore diameters of the products from the TTIP-dammar gum/$CHCl_3/H_2O$, TTIP-dammar gum/$CHCl_3$, and $TTIP/CHCl_3/H_2O$ reaction systems were 17.78 A°, 17.03 A°, and 17.01 A°, respectively. The physical properties of the TiO_2 with the large surface area make it a suitable candidate material for photocatalytic activity.

Rhodamine B (RhB) was chosen as the representative pollutant for the investigation of photocatalytic activity in the presence of the as-prepared TiO_2. The photocatalytic degradation of RhB was carried out under sunlight irradiation because using sunlight energy is economical and the procedure was suitable for large-scale reactions (Thite and Jadhav, 2017; Ariyanti et al., 2017). Figure 4 shows the resulting optical absorbance measurement of the RhB solutions using the UV-Vis spectrophotometer.

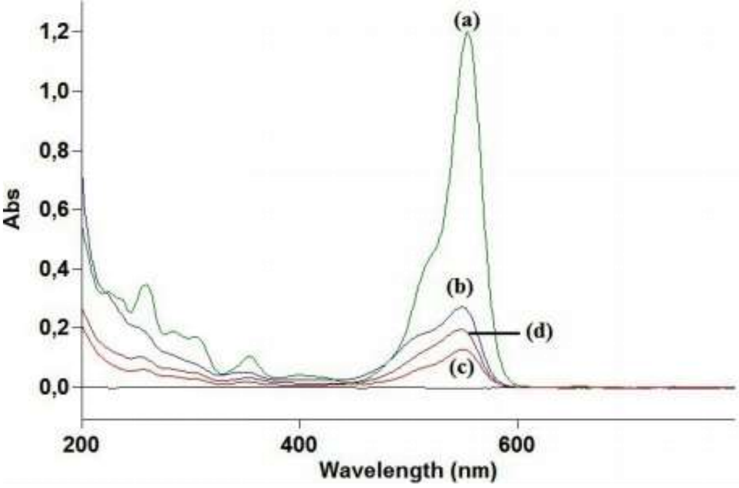

Figure 4 UV-Vis absorbance peak of: (a) pure RhB (5 ppm) after exposure to sunlight for 3 h; (b) RhB following exposure to sunlight and the addition of the TiO_2 obtained from the $TTIP/CHCl_3/H_2O$ reaction system; (c) RhB following exposure to sunlight and the addition of TiO_2 obtained from the TTIP-dammar gum/$CHCl_3/H_2O$ reaction system; (d) RhB following exposure to sunlight and addition of the TiO_2 obtained from the TTIP-dammar gum/$CHCl_3$ reaction system

Based on Figure 4, the presence of titania catalysts were important to reduce the RhB concentration, as judged by the absorbance value when using UV-Vis spectrophotometer. The absorbance of RhB decreased when the color intensity of the RhB decreased. Moreover, a blank sample that does not contain the TiO_2 catalyst was also measured under the same conditions in order to investigate possible auto-degradation under sunlight irradiation. The blank study revealed that photolysis of RhB did not take place. The main results showed that the TiO_2 obtained from the TTIP-dammar gum/$CHCl_3$/H_2O and TTIP-dammar gum/$CHCl_3$ reactions system possessed slightly better photocatalytic activity when degrading RhB (89.60% and 84.68%, respectively) than the titania that was isolated from the TTIP/$CHCl_3$/H_2O reaction system (78.36%). The reason for these differences could be explained by the fact that the surface areas of both types of TiO_2 (from TTIP-dammar gum/$CHCl_3$/H_2O and TTIP-dammar gum/$CHCl_3$ reaction systems) were in almost similar patterns. The mentioned results can be compared to TiO_2 produced using other methods (Jing et al., 2011; Zhao et al., 2016; Thite and Jadhav, 2017). In general, it was expected that it would be possible to successfully produce TiO_2 with good properties using natural templates, such as dammar gum, to improve the surface area and increase the activity of the corresponding photocatalyst. Based on surface area and photocatalytic activity, the reaction system that used dammar gum as a soft template followed by the addition of water was useful to obtain titania (TiO_2) with better performance.

4. Conclusions

In conclusion, we report the use of dammar gum as a soft template for the efficient preparation of crystalline photocatalysts with porous structures and large surface areas through the synthesis of anatase TiO_2. The described reaction conditions did not require the addition of any base or the use of high temperatures. Furthermore, the obtained product proved to be effective as a photocatalyst in rhodamine B degradation under sunlight irradiation. Further investigations of the obtained titania for other applications are on-going in our laboratory.

Acknowledgements

We are grateful to the Kementerian Riset, Teknologi dan Pendidikan Tinggi (Kemenristekdikti) Republic of Indonesia for its financial support under the World Class Professor (WCP) Program, fiscal year 2019.

References

Ariyanti, D., Maillot, M., Gao, W., 2017. TiO_2 Used as Photocatalyst for Rhodamine B Degradation under Solar Radiation. *International Journal of Modern Physics B,* Volume 31(16–19), pp. 1–5

Ba-Abbad, M.M., Kadhum, A.A.H., Mohamad, A.B., Takriff, M.S., Sopian, K., 2012. Synthesis and Catalytic Activity of TiO_2 Nanoparticles for Photochemical Oxidation of Concentrated Chlorophenols under Direct Solar Radiation. *International Journal of Electrochemical Science,* Volume 7, pp. 4871–4888

Bao, S.-J., Lei, C., Xu, M.-W., Cai, C.-J., Jia, D.Z., 2012. Environment-friendly Biomimetic Synthesis of TiO_2 Nanomaterials for Photocatalytic Application. *Nanotechnology,* Volume 23(20), pp. 1–7

Hernández-Gordillo, A., Campero, A., Vera-Robles, L.I., 2018. Mesoporous TiO_2 Synthesis using a Semi-hard Biological Template. *Microporous and Mesoporous Materials,* Volume 270, pp. 140–148

Ibrahim, A., Mekprasart, M., Pecharapa, W., 2017. Anatase/rutile TiO_2 Composite Prepared via Sonochemical Process and Their Photocatalytic Activity. *Materials Today: Proceedings*, Volume 4(5) Part 2, pp. 6159–6165

Jing, Z., Song, Y., Lu, F., Fei, W., Mengqiong, Y., Genxiang, L., Qian, X., Xiang, W., Can, L., 2011. Photocatalytic Degradation of Rhodamine B on Anatase, Rutile, and Brookite TiO_2, *Chinese Journal of Catalysis,* Volume 32(6–8), pp. 983 – 991

Kusrini, E., Putra, N., Siswahyu, A., Tristatini, D., Prihandini, W.W., Alhamid, M.I., Yulizar, Y., Usman, A., 2019. Effects of Sequence Preparation of Titanium Dioxide–Water Nanofluid using Cetyltrimethylammonium Bromide Surfactant and TiO_2 Nanoparticles for Enhancement of Thermal Conductivity. *International Journal of Technology*, Volume 10(7), pp. 1453–1464

Liu, L., Zhang, Y., Dong, S., Zhang, B., Meng, S., Xu, J., Gao, P., Feng, Y., 2018. Template Controlled Synthesis of Mesoporous TiO_2 Particles for Efficient Photoanodes in Dye Sensitized Solar Cells. *Journal of the Electrochemical Society*, Volume 165(2), pp. F1–F6

Morkhade, D.M., Joshi, S.B., 2007. Evaluation of Gum Dammar as Microencapsulating Material for Ibuprofen and Diltiazem Hydrochloride. *Indian Journal of Pharmaceutical Science*, Volume 69(2), pp. 263–268

Niu, B., Wang, X., Wu, K., He, X., Zhang, R., 2018. Mesoporous Titanium Dioxide: Synthesis and Applications in Photocatalysis, Energy and Biology. *Materials*, Volume 11(10), pp. 1910

Nursama, N.M., Muliani, L., 2012. Investigation of Photoelectrode Materials Influences in Titania-Based-Dye-Sensitized Solar Cells. *International Journal of Technology*, Volume 3(2), pp. 129–139

Ojeda, M., Chen, B., Leung, D.Y.C., Xuan, J., Wanga, H., 2017. A Hydrogel Template Synthesis of TiO_2 Nanoparticles for Aluminum-Ion Batteries. *Energy Procedia*, Volume 105, pp. 3997–4002

Osman, E.-b., Moriga, T., Murai, K.-I., Abd Rashid, M.W.-b., Manaf, M.E.A., Horikawa, T., 2018. Photocatalytic Activity of Nanostructured Tubular TiO_2 Synthesized using Kenaf Fibers as a Sacrificial Template. *Industrial Crops and Products,* Volume 113, pp. 210–221

Peng, Z., Li, H., Ba, X., Zhao, J., Sun, X., Li, Y., 2016. Synthesis of TiO_2 Nanoparticles in the PAMAM Hydrogen Network Template. *e-Polymers,* Volume 16(3), pp. 177–180

Ramimoghadam, D., Bagheri, S., Abd Hamid, S.B., 2014. Biotemplated Synthesis of Anatase Titanium Dioxide Nanoparticles via Lignocellulosic Waste Material. *BioMed Research International,* Volume 2014, pp. 1–7

Scarpelli, F., Mastropietro, T.F., Poerio, T., Godbert, N., 2018. Mesoporous TiO_2 Thin Films: State of the Art. *In*: Titanium Dioxide Material for a Sustainable Environment, pp. 57–80

Slamet, Oktrianto, Hendrasa, A., Ratnawati, Mustofa S., 2017. Photodegradation of Methylcyclohexane in Two Phases with Modified-Titania Immobilized on Pumice**.** *International Journal of Technology***,** Volume 8(1), pp. 27–36

Tang, G., Liu, S., Tang, H., Zhang, D., Li, C., Yang, C., 2013. Template-Assisted Hydrothermal Synthesis and Photocatalytic Activity of Novel TiO_2 Hollow Nanostructures. *Ceramics International*, Volume 39(5), pp. 4969–4974

Thite, T.M., Jadhav, S.M., 2017. Synthesis of TiO_2 Photocatalyst for Rhodamine B dye Degradation under Solar Light. *International Journal of Research in Applied Sciences and Engineering Technology*, Volume 5, pp. 2210– 2214

Tu, Y.D., Zhou, Z., Yan, R.J., Gan, Y.P., Huang, W.Z., Weng, X.X., Huang, H., Zhang, W.K., Tao, X.Y., 2012. Bio-template Synthesis of Spirulina/TiO_2 Composite with Enhanced Photocatalytic Performance. *RSC Advances*, Volume 2(28), pp. 10585–10591

Wang, J., Huang, D., Li, Z., Liu, G., Min, Y., 2015. Synthesis of TiO_2 with Cotton as Template and its Applications as Photocatalysis. *Asian Journal of Chemistry*, Volume 27(1), pp. 243–245

Xie, Y., Kocaefe, D., Chen, C., Kocaefe, Y., 2016. Review of Research on Template Methods in Preparation of Nanomaterials. *Journal of Nanomaterials*, Volume 2016, pp. 1–10

Xiong, Z., Dou, H., Pan, J., Ma, J., Xu, C., Zhao, X.S., 2010. Synthesis of Mesoporous Anatase TiO_2 with a Combined Template Method and Photocatalysis. *CrystEngComm*, Volume 12(11), pp. 3455–3457

Yang, X., Ma, P., Qi, H., Zhao, J., Wu, Q., You., J., Li, Y., 2017. TiO_2 Nanotube Arrays: Fabricated by Soft–Hard Template and the Grain Size Dependence of Field Emission Performance. *Nanoscale Research Letter,* Volume 12(1), pp. 593–598

Yu, C., Li, X., Liu, Z., Yang, X., Huang, Y., Lin, J., Zhang, J., Tang, C., 2016. Synthesis of Hierarchically Porous TiO_2 Nanomaterials using Alginate as Soft Templates. *Materials Research Bulletin,* Volume 83, pp. 609–614

Zhang, Z., Zuo, F., Feng, P., 2010. Hard Template Synthesis of Crystalline Mesoporous Anatase TiO_2 for Photocatalytic Hydrogen Evolution. *Journal of Material Chemistry*, Volume 20(11), pp. 2206–2212

Zhang, H., Dong, F., Zhai, S., Kang, X., Fan, S., 2012. Preparation of Ordered TiO_2 Macroporous Membrane using PBMA Colloid Crystal as Template. *Advanced Materials Research*, Volume 399–401, pp. 677–682

Zhang, X., Jing, S., Chen, Z., Zhong, L., Liu, Q., Peng, X., Sun, R., 2017. Fabricating 3D Hierarchical Porous TiO_2 and SiO_2 with High Specific Surface Area by using Nanofibril-Interconnected Cellulose Aerogel as a New Biotemplate. *Industrial Crops and Products*, Volume 109, pp. 790–802

Zhao, T., Ren, Y., Yang, J., Wang, L., Jiang, W., Elzatahry, A.A., Alghamdi, A., Deng, Y., Zhao, D., Luo, W., 2016. Hierarchical Ordered Macro/Mesoporous Titania with a Highly Interconnected Porous Structure for Efficient Photocatalysis. *Journal of Material Chemistry A*, Volume 4(42), pp. 16446–16453

Zulmajdi, S.L.N., Zamri, N.I.I., Yasin, H.M., Kusrini, E., Hobley, J., Usman, A., 2020. Comparative Study on the Adsorption, Kinetics, and Thermodynamics of the Photocatalytic Degradation of Six Different Synthetic Dyes on TiO_2 Nanoparticles. *Reaction Kinetics, Mechanisms and Catalysis*, Volume 129(1), pp. 519–534